

Radiative Transfer in the Midwave Infrared Applicable to Full Spectrum Atmospheric Characterization

Michael Griffin, Hsiao-hua Burke, John Kerekes
MIT Lincoln Laboratory
Lexington, MA

Abstract— The compensation for atmospheric effects in the VNIR/SWIR has reached a mature stage of development with many algorithms available for application (ATREM, FLAASH, ACORN, etc.). Compensation of LWIR data is the focus of a number of promising algorithms. A gap in development exists in the MWIR where little or no atmospheric compensation work has been done yet an increased interest in MWIR applications is emerging. To obtain atmospheric compensation over the full spectrum (visible through LWIR), a better understanding of the radiative effects in the MWIR is needed. The MWIR is characterized by a unique combination of reduced solar irradiance and low thermal emission (for typical emitting surfaces), both providing relatively equal contributions to the daytime MWIR radiance. In the MWIR and LWIR, the compensation problem can be viewed as two interdependent processes: compensation for the effects of the atmosphere and the uncoupling of the surface temperature and emissivity. The former requires calculations of the atmospheric transmittance due to gases, aerosols, and thin clouds and the path radiance directed towards the sensor (both solar scattered and thermal emissions in the MWIR). A framework for a combined MWIR/LWIR compensation approach is presented where both scattering and absorption by atmospheric particles and gases are considered.

Keywords: MWIR, LWIR, hyperspectral, atmospheric compensation, radiative transfer

I. INTRODUCTION

Hyperspectral imaging sensors have been used to aid in the detection and identification of diverse surface elements, topographical, and geological features, ambient dust and aerosols, smoke from fires, as well as suspended gaseous effluents. Hyperspectral data are not immune to the effects of the intervening atmosphere. The term “atmospheric compensation” refers to the removal of unwanted atmospheric components of the measured radiance so that an estimate of the surface leaving radiance or reflectance can be obtained. For hyperspectral data analysis in the reflected solar spectral regime, the general objective of atmospheric compensation algorithms is to remove solar illumination and atmospheric effects (predominantly aerosol scattering and water vapor

absorption) from the measured spectral data so that an accurate estimate of the surface reflectance can be obtained [1]. In the thermal emissive region of the spectrum, the objective is two-fold: 1) remove atmospheric components of the sensor-measured radiance to obtain a ground-leaving radiance, and 2) separate the temperature and emissivity components from the retrieved radiance [2], the final goal being an estimate of the surface spectral emissivity.

Difficulties can arise when atmospheric conditions are stressing (e.g., high moisture, heavy aerosol/particulate loading, partial cloud cover, low sun angle). These effects are further enhanced when the measured signal is low (over low reflectance or cold surfaces or for spectral regions of low solar or thermal radiance). In the MWIR (3 – 6 μm), the reflected solar radiance is quite small compared to that in the VNIR and the thermal emissive radiance for normal surface and atmospheric conditions is also at a minimum. These factors provide a unique challenge to those who attempt to derive information from MWIR data. The following sections will highlight the typical spectral and radiometric signatures to be found in the MWIR for different scenarios. The equations governing the transfer of radiation in this regime will also be examined.

II. MWIR SPECTRAL CHARACTERISTICS

To estimate the underlying surface-leaving radiance from a remote airborne or spaceborne platform, the effects of the intervening atmosphere must be considered. Typically, at MWIR wavelengths, the radiative flux is impacted by the absorption by well-mixed gases such as Ozone (O_3), Oxygen (O_2), Nitrogen (N_2), Methane (CH_4), Nitrous Oxide (N_2O), Nitrogen Dioxide (NO_2) and Carbon Dioxide (CO_2), and the absorption by water vapor. Mixed gases can be modeled accurately and play an important role in the retrieval of specific properties of the earth-atmosphere system [3].

Figure 1 provides examples of the atmospheric absorption (defined as $1 - \text{transmittance}$) over the spectral region from 2.5 to 6 μm for two atmospheric conditions: 1) clear and dry and 2) hazy and humid. The curves were produced with Modtran [4] over a full (100 km) nadir atmospheric path. These cases produce values for atmospheric absorption that represent the extreme bounds for a nominal atmosphere. It is clear that the MWIR spectral band is dominated by strongly absorbing gases.

This work was sponsored by the Department of Defense under Air Force Contract F19628-00-C-0002. Opinions, interpretations, conclusions and recommendations are those of the authors and not necessarily endorsed by the United States Government.

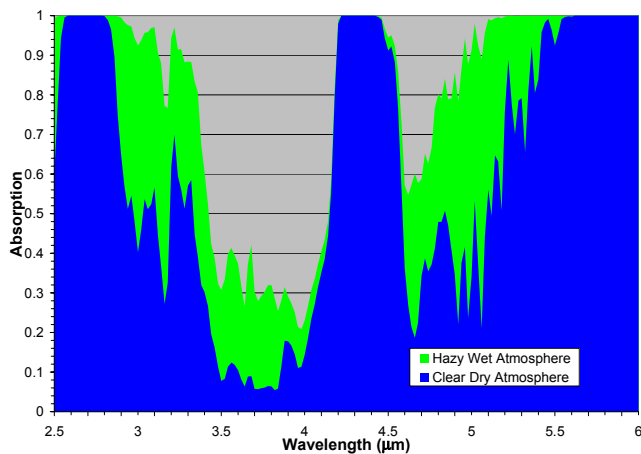


Figure 1. Plot of the atmospheric absorption across the MWIR spectral region for two atmospheric conditions: hazy and wet and clear and dry.

One moderately transmissive “window” region exists between 3 and 4 microns with minimum absorption near 3.8 μm for dry atmospheres and 3.9 μm for moist atmospheres. A second transmissive region exists between 4.6 and 5.4 μm with minimum absorption values near 4.6 μm . In contrast with the VNIR/SWIR spectral band, which exhibits numerous atmospheric windows, the MWIR has limited spectral regions for retrieving surface information.

Scattering by molecules is negligible at these wavelengths [5], and scattering and absorption by normal atmospheric aerosols produces transmission losses between 2 and 15 percent depending on the aerosol type and visibility. Typical absorption loss based on Modtran aerosol modeling is limited to 1 – 4 percent with minimum absorption occurring for maritime aerosols and maximum absorption found in urban aerosols that tend to contain significant amounts of carbon. The scattering from aerosols is found to vary slowly and continuously with wavelength with a slight decrease in transmission loss towards longer wavelengths in the MWIR. Models have been developed based upon the size and near-spherical shape of aerosols to estimate their effects on the transmission of solar and thermal energy in the atmosphere [6].

III. MWIR RADIOMETRIC CHARACTERISTICS

The MWIR spectral region is unique in that it is not situated near the peak of a source of emission. In the VNIR, scattering of the sun’s energy by the earth-atmosphere system dominates the radiative transfer; thermally emitted radiance is negligible for almost all conditions (fires can be an exception [7]). The opposite is true for the LWIR, where the thermal emission from the earth and atmosphere dominate. Solar radiation has no component in the transfer of radiation in the LWIR, however, the absorption of solar radiation by the earth and the atmosphere will alter the temperature and the resultant re-emission in the LWIR. Between the two spectrums where contributions from both sources are important, the radiative

transfer is more complex with both scattering and absorption effects needing consideration.

Figure 2 provides a plot of the individual components of the radiative transfer: surface emitted thermal radiance, surface reflected downwelling solar radiance, thermal path radiance, and reflected path solar radiance. The magnitude of each component is shown as a fraction of the total radiance received at the TOA. The left plot represents values for dry and clear atmospheric conditions and the plot on the right for a wet and hazy scene. The magnitude of both the solar and thermal path radiances is a direct result of the amount of atmospheric absorption and scattering, primarily from water vapor and aerosols, respectively. Both radiance components increase with increasing humidity and aerosol turbidity. The surface components (reflected solar and infrared and thermal emitted) are also affected, but in a different manner. The transmission of the surface emitted radiance is attenuated more for a murkier path, as is the downwelling radiance reflected by the surface back towards the sensor. For the MWIR window region (3.4 – 4.1 μm), the TOA radiance is dominated by the surface components, which make up from 80 - 95% of the total radiance depending on the atmospheric conditions. The remaining 5 – 20% is due to the path thermal emissions with a small amount from scattered solar radiation. Beyond the CO₂ absorption band, the contribution to the TOA radiance from surface-reflected solar or thermal radiation is very small even for very dry conditions (less than 2% at 5 μm).

IV. MWIR RADIATIVE TRANSFER

The transfer of radiation in the MWIR must include both solar reflected and thermal emitted components. Separate equations can be written for each radiance source. For clear-sky conditions, assuming a plane-parallel atmosphere and a Lambertian surface, the upwelling radiance at the sensor (or TOA) L_S^m due to scattered solar radiation can be expressed by [8]

$$L_S^m = L_S^\uparrow + \frac{(1 - \epsilon_s) L_S^\downarrow t}{1 - S(1 - \epsilon_s)}, \quad (1)$$

where L_S^\uparrow is the scattered path radiance at the sensor and L_S^\downarrow is the total (diffuse and direct) solar radiance that reaches the surface, ϵ_s is the surface emissivity, t is the atmospheric transmittance for the surface to sensor path and S is the spherical albedo. A dependence on wavelength is assumed for each parameter. The two terms on the right-hand side of (1) represent the scattered path radiance and the surface reflected radiance. The direct component of the downwelling solar radiance at the surface is given by the formula,

$$L_{S,dir}^\downarrow = \frac{F_0}{\mu_0 d_m^2} t_0. \quad (2)$$

Here F_0 is the solar radiance at the TOA, μ_0 is the cosine of the solar zenith angle, d_m is the earth-sun distance ratio and t_0 is the transmission from the TOA to the surface along the sun to surface path. The diffuse component of the downwelling solar radiance is due to multiple scattering by atmospheric molecules

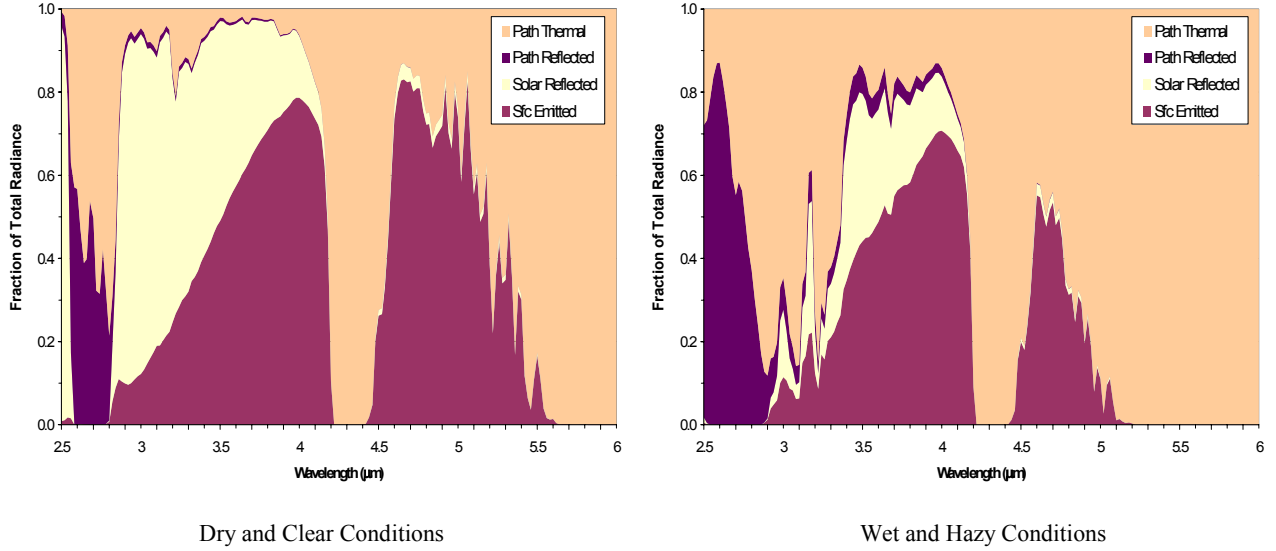


Figure 2. Plots of the four radiance components for the two sets of atmospheric conditions are shown. The plots depict the fraction of the total radiance for each component displayed in a stacked plot.

and particulates and can be computed by multiple scattering codes such as DISORT n -stream [9], which is packaged with Modtran.

For thermally emitted and absorbed radiation, using the same assumptions as before, the upwelling radiance at the sensor (or TOA) L_T^m under clear-sky conditions can be expressed by [10],

$$L_T^m = \varepsilon_s B[T_s] t + L_T^\uparrow + (1 - \varepsilon_s) L_T^\downarrow t \quad (3)$$

In (3) L_T^\uparrow is the thermal path radiance at the sensor and L_T^\downarrow is the downwelling radiance at the surface, B is the Planck function, and T_s is the surface skin temperature. As before all parameters have a dependence on wavelength. The three terms on the right-hand side of (3) represent the surface emitted thermal radiation, the path radiance, and the reflected downwelling thermal radiance components of the total measured radiance at the sensor, respectively. Equations (1) and (3) can be combined to provide the total radiance received at the sensor (or TOA),

$$L^m = (L_T^\uparrow + L_S^\uparrow) + t \left\{ \varepsilon_s B[T_s] + (1 - \varepsilon_s) \left(L_T^\downarrow + \frac{L_S^\downarrow}{1 - S(1 - \varepsilon_s)} \right) \right\} \quad (4)$$

The first term on the right is the total path radiance from both scattered solar and thermal emitted components. The second term is the radiance from the surface either from thermal emission or from reflection of downwelling solar or thermal radiation. Therefore the total upwelling radiance for the MWIR can be divided into three components, the path radiance, the surface emitted and surface reflected downwelling radiance.

V. ATMOSPHERIC COMPENSATION

In the VNIR/SWIR spectral region where reflected solar radiance is the primary source of radiant energy, the primary product of atmospheric compensation models is to recover the spectral surface reflectance. For spectral regions dominated by infrared radiative transfer, the primary product of atmospheric compensation models is still the surface reflectance (or more commonly the surface emissivity), however, the complex relationship between surface emissivity and temperature requires an extra step in the atmospheric compensation process. The first step retrieves the surface-leaving radiance by compensating for atmospheric effects in a manner similar to that used in the VNIR/SWIR. The surface-leaving radiance can be defined as,

$$L_{sfc} = \varepsilon_s B[T_s] + (1 - \varepsilon_s) L^\downarrow \quad (5)$$

Here, L^\downarrow represents the total solar and thermal downwelling radiance at the surface. The second step requires the separation of the temperature and emissivity components of L_{sfc} using one of many techniques appropriate to the type of sensor making the measurements [2][11].

From Fig. 2, it is apparent that some terms in (4) contribute more to the overall at-sensor radiance than others. The path-reflected solar radiance and the surface-reflected downwelling thermal radiance together provide between 1 and 4 percent of the radiance received at the sensor in the MWIR window. Below 3 μm , the path reflected solar radiance appears to provide a significant contribution but due to the very small source radiance this contribution is essentially negligible. Neglecting these two terms for now, we can simplify (4) slightly,

$$L^m \cong L_T^\uparrow + t \varepsilon_s B[T_s] + \frac{t(1-\varepsilon_s)L_S^\downarrow}{1-S(1-\varepsilon_s)}, \quad (6)$$

For this spectral region, there are now three terms that combine to approximate the at-sensor radiance: the path thermal (5-18%), the surface emitted (56-65%) and the reflected downwelling solar radiance (22-30%), with relative contributions to the MWIR window at-sensor radiance shown in parenthesis. Beyond the 4.25 μm CO_2 band, the solar component diminishes so the third term in (5) can be neglected,

$$L^m \cong L_T^\uparrow + t \varepsilon_s B[T_s], \quad \lambda > 4.5 \mu\text{m}. \quad (7)$$

Equation (6) contains two thermal radiance terms plus a solar reflectance term, from which the surface leaving radiance can be estimated,

$$L_{sfc} = \varepsilon_s B[T_s] + (1-\varepsilon_s)L^\downarrow = \frac{L^m - L_T^\uparrow}{t}. \quad (8)$$

The quantity L_{sfc} represents the total surface leaving radiance, a combination of the thermal emitted and downwelling solar and thermal radiance. The unknowns in computing L_{sfc} are the upwelling thermal radiance at the sensor and the atmospheric transmission. Spectral values for these variables can be estimated from radiative transfer model calculations using scene appropriate model inputs to obtain an estimate of the total surface leaving radiance in the MWIR.

From (8), an estimate of the surface emissivity can be obtained,

$$\varepsilon_s = \frac{L_{sfc} - L^\downarrow}{B[T_s] - L^\downarrow}. \quad (9)$$

Here, the key unknown is the surface temperature.

VI. SUMMARY

The spectral and radiometric characteristics of radiative transfer in the MWIR have been examined. The effects of mixed gases are numerous in the MWIR, although much of the spectral region is dominated by water vapor and carbon dioxide absorption. Aerosols were found to still have an influence in

the MWIR and should be included in any radiative transfer calculations. Combining radiative transfer equations for both the solar reflective and the thermal emissive regimes, and neglecting terms that provided minimal contributions to the overall at-sensor radiance, the expected at-sensor radiance could be estimated. From this a simplified equation for the surface-leaving radiance (both solar and thermal components) was derived. Limited availability of MWIR data precluded application of the equation at this time.

REFERENCES

- [1] Griffin, M.K. and H.K. Burke, "Compensation of Hyperspectral Data for Atmospheric Effects," *Lincoln Laboratory Journal*, **14**, pp. 29-54, 2003.
- [2] Caselles, V., E. Valor, C. Coll, and E. Rubio, "Thermal band selection for the PRISM instrument 1. Analysis of emissivity-temperature separation algorithms," *J. Geophys. Res.*, **102**, 11145-11164, 1997.
- [3] Malkmus, W., 1967: Random Lorentz band model with exponential-tailed S line intensity distribution function. *J. Opt. Soc. Am.*, **57**, 323-329.
- [4] Berk, A., L.S. Bernstein, G.P. Anderson, P.K. Acharya, D.C. Robertson, J.H. Chetwynd, and S.M. Adler-Golden, "MODTRAN Cloud and Multiple Scattering Upgrades with Application to AVIRIS," *Remote Sens. Environ.*, **65**, pp. 367-375, 1998.
- [5] McCartney, E.J.: Optics of the Atmosphere; Scattering by Molecules and Particles. John Wiley & Sons, New York, NY, 408 pp.
- [6] Shettle, E.P., and R.W. Fenn, 1979: Models for the Aerosols of the Lower Atmosphere and the Effects of Humidity Variations on Their Optical Properties. *AFGL TR 79-0214*, Air Force Geophysics Laboratory, Hanscom AFB, MA, 94 pp.
- [7] Griffin, M.K., S.M. Hsu, H.K. Burke, and J.W. Snow, "Characterization and Delineation of Plumes, Clouds and Fires in Hyperspectral Images," *SPIE* **4049**, 274-283, 2000.
- [8] Vermote, E.F., N. El Saleous, C.O. Justice, Y.J. Kaufman, J.L. Privette, L. Remer, J.C. Roger and D. Tanre, "Atmospheric Correction of Visible to Middle-Infrared EOS-MODIS Data Over Land Surfaces: Background, Operational Algorithm and Validation," *J. Geophys. Res.*, **102**, 17131-17141, 1997.
- [9] Stamnes, K., S.-C. Tsay, W. Wiscombe and K. Jayaweera, "Numerically Stable Algorithm For Discrete-Ordinate-Method Radiative Transfer In Multiple Scattering and Emitting Layered Media," *Appl. Opt.*, **27**, 2502-2509, 1988.
- [10] Gu, D., A.R. Gillespie, A.B. Kahle, and F.D. Palluconi, "Autonomous Atmospheric Compensation (AAC) of High Resolution Hyperspectral Thermal Infrared Remote-Sensing Imagery," *IEEE Trans. on Geos. & Rem. Sens.*, **38**, 2557-2570, 2000.
- [11] Becker, F., "The impact of spectral emissivity on the measurement of land surface temperature from a satellite," *Int. J. Remote Sens.*, **11**, 369-394, 1987.